VACCINES

Synthetic Generation of Influenza Vaccine Viruses for Rapid Response to Pandemics

Philip R. Dormitzer,[1]* Pirada Suphaphiphat,[1] Daniel G. Gibson,[2,3,4] David E. Wentworth,[2] Timothy B. Stockwell,[2] Mikkel A. Algire,[2] Nina Alperovich,[2] Mario Barro,[5] David M. Brown,[2] Stewart Craig,[1] Brian M. Dattilo,[5] Evgeniya A. Denisova,[2] Ivna De Souza,[1] Markus Eickmann,[6] Vivien G. Dugan,[2†] Annette Ferrari,[1] Raul C. Gomila,[1,7] Liqun Han,[1] Casey Judge,[1] Sarthak Mane,[1] Mikhail Matrosovich,[6] Chuck Merryman,[3] Giuseppe Palladino,[1] Gene A. Palmer,[1] Terika Spencer,[1,8] Thomas Strecker,[6] Heidi Trusheim,[8] Jennifer Uhlendorff,[6] Yingxia Wen,[1] Anthony C. Yee,[2] Jayshree Zaveri,[2] Bin Zhou,[2] Stephan Becker,[6] Armen Donabedian,[5] Peter W. Mason,[1] John I. Glass,[2] Rino Rappuoli,[1,7] J. Craig Venter[2,3,4]

During the 2009 H1N1 influenza pandemic, vaccines for the virus became available in large quantities only after human infections peaked. To accelerate vaccine availability for future pandemics, we developed a synthetic approach that very rapidly generated vaccine viruses from sequence data. Beginning with hemagglutinin (HA) and neuraminidase (NA) gene sequences, we combined an enzymatic, cell-free gene assembly technique with enzymatic error correction to allow rapid, accurate gene synthesis. We then used these synthetic HA and NA genes to transfect Madin-Darby canine kidney (MDCK) cells that were qualified for vaccine manufacture with viral RNA expression constructs encoding HA and NA and plasmid DNAs encoding viral backbone genes. Viruses for use in vaccines were rescued from these MDCK cells. We performed this rescue with improved vaccine virus backbones, increasing the yield of the essential vaccine antigen, HA. Generation of synthetic vaccine seeds, together with more efficient vaccine release assays, would accelerate responses to influenza pandemics through a system of instantaneous electronic data exchange followed by real-time, geographically dispersed vaccine production.

INTRODUCTION

The response to the 2009 H1N1 influenza pandemic was the fastest global vaccine development effort in history. Within 6 months of the pandemic declaration, vaccine companies had developed, produced, and distributed hundreds of millions of doses of licensed pandemic vaccines. Unfortunately, the response was not fast enough. Substantial vaccine quantities were available only after the second pandemic wave had peaked (*1*). Manufacture of influenza virus subunit vaccines requires a vaccine virus that grows well enough in eggs or cultured mammalian cells to produce sufficient amounts of the essential vaccine antigen, hemagglutinin (HA), to meet vaccine needs. Late availability of a high-yielding vaccine virus contributed to the delay in vaccine supply.

In parallel with other efforts (*2*, *3*), Novartis Vaccine and Diagnostics (NV&D) used recombinant DNA methods to generate a potential vaccine virus on a standard [A/Puerto Rico/8/1934 (H1N1) (PR8)] vaccine backbone on 11 May 2009, 11 days after receiving influenza strain A/California/04/2009 (H1N1) viral RNA from the U.S. Centers for Disease Control (CDC) (figs. S1A and S2, A to C). In contrast, NV&D first received a conventional reassortant vaccine virus (X179A) from a World Health Organization (WHO) Collaborating Center at one of its vaccine manufacturing facilities on 29 May, 18 days after we had generated our potential vaccine virus with recombinant methods (fig. S1A). Adaptation of the research-based process of recombinant vaccine virus generation to one that used a manufacturing-qualified cell line and good manufacturing practice (GMP) standards was completed at the Philipps-Universität Marburg on 1 June 2009, 3 days after receipt of X179A (*4*, *5*) (fig. S1A). Our recombinant vaccine virus was not used to produce the vaccines that were distributed to the public in the 2009 pandemic response because the regulatory hurdles for using a new process to produce an urgently needed vaccine were too great. Instead, although the yield of HA from X179A was only 30 to 50% of the yield from H1N1 vaccine viruses typically used for seasonal vaccine manufacture (*2*), the pandemic vaccine manufacturing campaign was initiated with an X179A-derived vaccine seed virus.

This experience with the 2009 H1N1 virus provided lessons for the next pandemic vaccine response: (i) Synthetic genomics techniques to produce influenza genome segments rapidly, accurately, and reliably are needed, so that instantaneous exchange of electronic sequence data followed by local gene synthesis can replace the isolation of viruses, preparation of high-growth reassortant vaccine viruses, and shipment of viruses and nucleic acids between geographically dispersed sites where vaccines are manufactured. (ii) A reverse genetics system that uses these synthesized genes to generate viruses that are suitable for use in GMP-compliant vaccine manufacturing should be in place. (iii) To increase the reliability of generating high-yielding, antigenically correct vaccine viruses, a greater variety of influenza HA and neuraminidase (NA) variants should be rescued in the context of multiple combinations of other influenza genome segments. (iv) The use of synthetic and reverse genetic technologies for pandemic responses

[1]Novartis Vaccines and Diagnostics, Cambridge, MA 02139, USA. [2]The J. Craig Venter Institute, Rockville, MD 20850, USA. [3]The J. Craig Venter Institute, San Diego, CA 92121, USA. [4]Synthetic Genomics Inc., La Jolla, CA 92037, USA. [5]Biomedical Advanced Research and Development Authority, U.S. Department of Health and Human Services, Washington, DC 20201, USA. [6]Institut für Virologie, Philipps-Universität Marburg, D-35032 Marburg, Germany. [7]Novartis Vaccines and Diagnostics, 53100 Siena, Italy. [8]Novartis Vaccines and Diagnostics, Holly Springs, NC 25740, USA.
*Corresponding author. E-mail: philip.dormitzer@novartis.com
†Present address: Division of Microbiology and Infectious Diseases, National Institute of Allergy and Infectious Diseases, National Institutes of Health, U.S. Department of Health and Human Services, Bethesda, MD 20892, USA.

in seasonal influenza vaccine manufacture could establish regulatory and public acceptance and familiarity to allow reliable application of these approaches during a public health emergency.

On the basis of these lessons and the U.S. government's interest in improving the influenza vaccine manufacturing enterprise, NV&D, the J. Craig Venter Institute (JCVI), Synthetic Genomics Vaccines Inc. (SGVI), and the Biomedical Advanced Research and Development Authority (BARDA), U.S. Department of Health and Human Services, initiated a collaboration to develop a rapid process for synthetic vaccine virus generation. We addressed three major technical barriers to more rapid and reliable pandemic responses: the speed of synthesizing DNA cassettes to drive production of influenza RNA genome segments, the accuracy of rapid gene synthesis, and the yield of HA from vaccine viruses.

RESULTS

Enzymatic assembly and in vitro error correction

We adapted an enzymatic one-step, isothermal assembly method for gene assembly, previously used to synthesize the 16,299–base pair (bp) mouse mitochondrial genome from 600 overlapping oligonucleotides (*6*), to generate synthetic DNA copies of influenza virus genome segments. 5′ T5 exonuclease, Phusion DNA polymerase, and Taq DNA ligase were used to join multiple DNA fragments during a brief 50°C reaction (*7*) (Fig. 1). We selected this method to assemble genes for our synthetic vaccine seeds because it is rapid and readily automated.

When phosphoramidite chemistry is used to build the precursor oligonucleotides of synthetic DNA constructs, one error per 500 to 750 bp is generally observed (with some variation between oligonucleotide manufacturers) (*6*). During the mouse mitochondrial genome synthesis, subassemblies of less than 500 bp were cloned and sequenced, and sets of error-free sequences were selected for subsequent rounds of assembly (*6*). Each cycle of synthesis, assembly, cloning, and sequencing that was required to collect a complete set of correct sequence fragments lasted 2 to 3 days, depending on the time needed for sufficient *Escherichia coli* growth for colony formation and plasmid preparation (Fig. 2A). For rapid influenza vaccine seed virus generation, we felt that this method of error correction would introduce unnecessary delays. However, when DNA copies of the 1.7-kb HA and 1.5-kb NA viral RNA genome segments were assembled with oligonucleotides about 60 bases in length with 30 bases of overlap between oligonucleotides on opposite strands without cloning and sequencing steps to select subassemblies without errors, an average of 3% of the assembled products had the correct sequence (1 of 48 HA clones and 2 of 48 NA clones).

We solved the problem of synthesizing DNA copies of HA and NA genome segments with both accuracy and speed by (i) increasing the overlap between oligonucleotides, (ii) introducing an enzymatic error correction step, and (iii) increasing the number of oligonucleotides assembled at once, eliminating the need for stepwise assembly via subassemblies (Fig. 1, A and B). Specifically, the length of oligonucleotides was increased to 60 to 74 bases, and full-length genes [including 5′ and 3′ untranslated regions (UTRs)] were assembled from staggered sets of oligonucleotides that contained all residues of a double-stranded

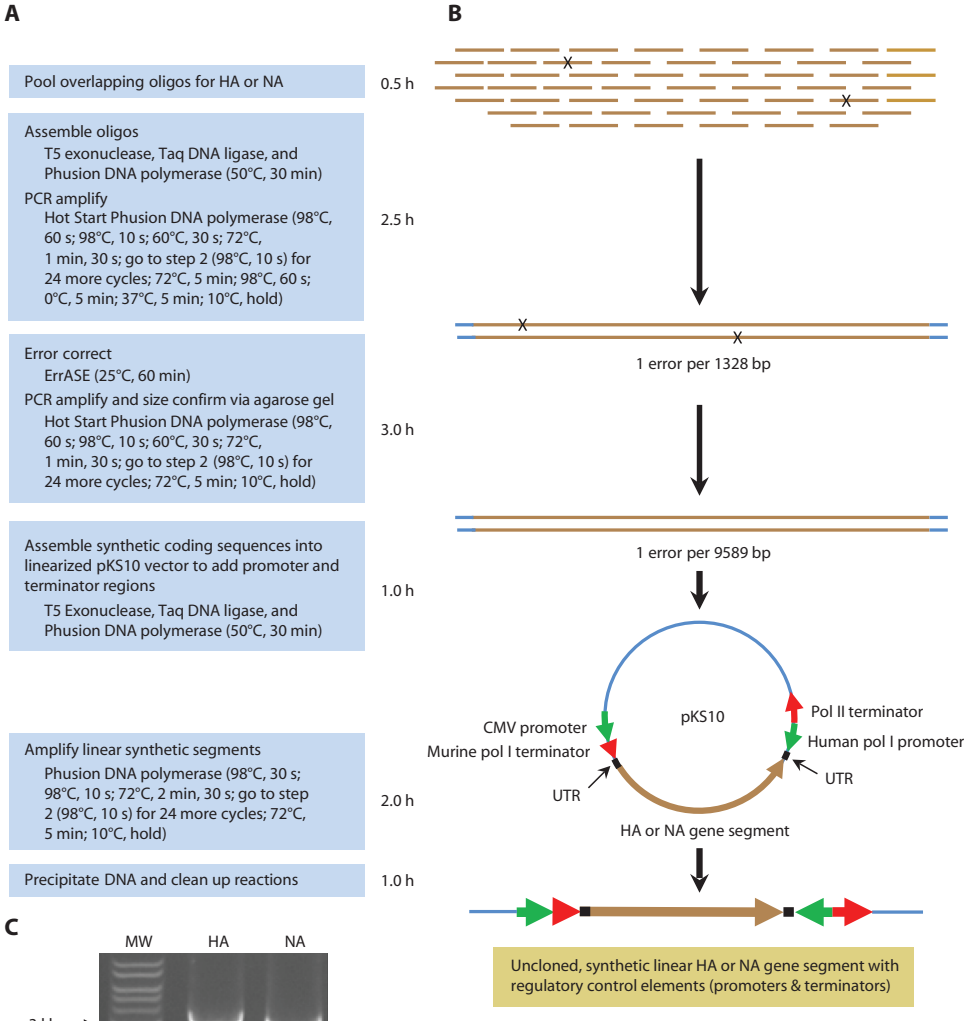

Fig. 1. Synthetic gene segment assembly and error correction. (**A**) Procedure for synthesis of HA and NA gene segments. (**B**) Schematic diagram of procedure in (A). X, sites of oligonucleotide synthesis errors. Brown, influenza coding sequences; blue, pKS10 sequences; green, promoter sequences; red, terminator sequences; black, UTRs. (**C**) Synthesized HA and NA genes. Two micrograms each lane of linear HA and NA genes separated by agarose gel electrophoresis, stained with ethidium bromide. MW, molecular weight marker.

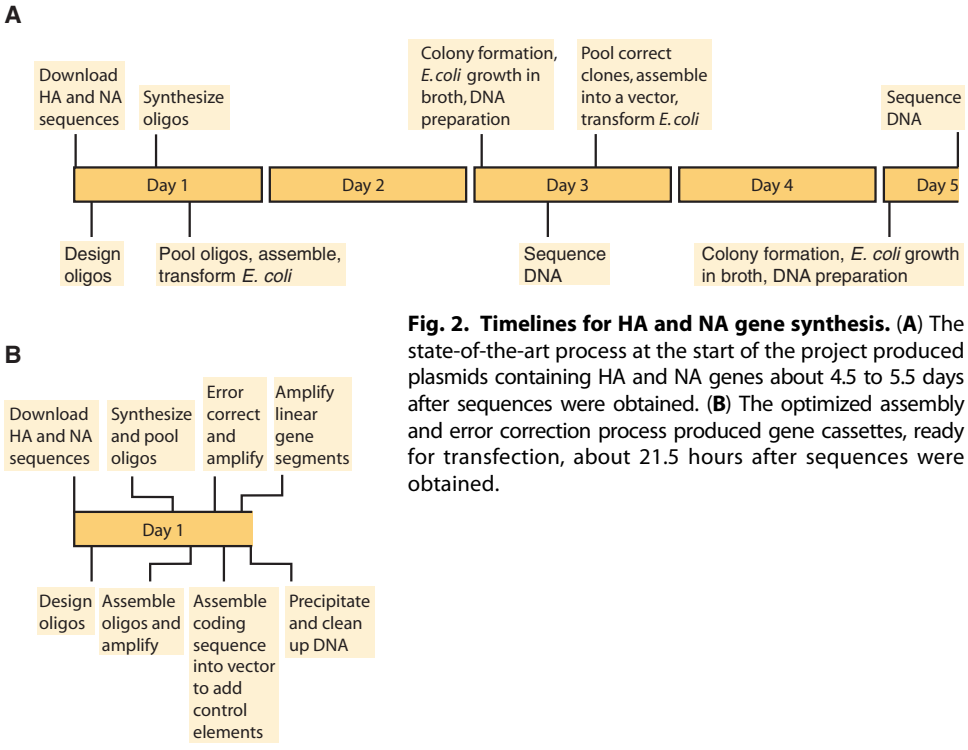

Fig. 2. Timelines for HA and NA gene synthesis. (**A**) The state-of-the-art process at the start of the project produced plasmids containing HA and NA genes about 4.5 to 5.5 days after sequences were obtained. (**B**) The optimized assembly and error correction process produced gene cassettes, ready for transfection, about 21.5 hours after sequences were obtained.

DNA molecule so that, before ligation, the full double-stranded gene could be annealed. In practice, the HA and NA BARDA Oligo Designer (HANABOD) software program generates a set of sequences for oligonucleotides (a maximum of 96 oligonucleotides per HA-NA pair to fit in a 96-well plate) that meet these criteria. After chemical synthesis of the oligonucleotides, enzymatic isothermal assembly, and polymerase chain reaction (PCR) amplification, error-containing DNA was removed enzymatically by treating melted and reannealed DNA with a commercially available error correction kit that excises areas of base mismatch in double-stranded DNA molecules before another round of PCR amplification.

After the products' sizes were verified on agarose gels (Fig. 1C), we added the control sequences [including polymerase I (Pol I) and Pol II promoters and their terminator and polyadenylation signals] needed to generate RNA genome segments and mRNA for virus rescue by isothermally coupling the synthetic DNA with a linearized plasmid (pKS10) that contained these regulatory sequences (*8*). Nucleotide identity between the ends of the linearized plasmid and the 5′ and 3′ primers used for gene synthesis guided this assembly. The assembled molecule was then used as the substrate for a round of high-fidelity PCR amplification with primers from outside the transcription control regions.

After purification and concentration of the amplicons, we obtained about 10 μg of assembled linear DNA cassettes that contained the influenza HA or NA gene flanked by control sequences and that were ready for transfection into the Madin-Darby canine kidney (MDCK) 33016PF cell line for influenza virus rescue. The time from receipt of oligonucleotides to a purified HA- or NA-encoding DNA cassette ready for transfection was about 10 hours (Figs. 1, A and B, and 2B). While virus rescue was under way with the enzymatically assembled, error-corrected, and amplified DNA, we verified the sequence of the assembled genes by cloning and sequencing. When we applied one round of enzymatic error correction, the rate of sequence errors in synthesized genes was <1 in 9000 bp, and ≥80% of the full-length HA and NA gene sequences obtained were correct (Table 1). This gene synthesis and assembly method enabled the rapid and accurate conversion of digitally transmitted sequence information to biologically active DNA genes.

Rescue of synthetic influenza viruses in a manufacturing cell line

The rescue protocol for synthetic seed virus generation is adapted from a previously described eight-plasmid ambisense system in which each expression plasmid has a complementary DNA (cDNA) copy of a viral gene segment bounded at the 5′ end by a Pol II promoter to drive transcription of messenger RNA and at the 3′ end by a human Pol I promoter to drive transcription of negative-stranded influenza RNA genome segments (*9*). The manufacturing-qualified MDCK 33016PF cell line is a less efficient substrate for transfection and influenza virus rescue by reverse genetics than 293T cells (which are not qualified for vaccine production). Reverse genetic rescue of influenza virus has been described in Vero cells (some banks of which are qualified for vaccine production) (*10*, *11*). However, using one cell line for vaccine virus rescue and a different cell line for antigen production would add adventitious agent risk and regulatory and manufacturing complexity. We therefore elected to increase the efficiency of reverse genetic DNA rescue in MDCK 33016PF cells so that a single cell line could be used for seed generation and vaccine antigen production. Although Pol I promoters are generally species-specific (*12*, *13*), human Pol I efficiently drives transcription in MDCK 33016PF cells, which are of canine origin (*14*).

One microgram of each linear synthetic cassette that encodes HA or NA was cotransfected into MDCK 33016PF cells together with 1 μg of each ambisense plasmid that encodes PA, PB1, PB2, NP, NS, or M and a helper plasmid that encodes the protease TMPRSS2 (*15*). To increase rescue efficiency, we added cultures of fresh (untransfected) MDCK 33016PF cells and additional TrypZean after transfection (*14*). Adding fresh cells after transfection increases the efficiency of virus recovery from DNA-transfected cells, presumably by providing a healthier population of cells in which rescued viruses can further amplify (fig. S3). Viruses were detected in cell culture medium within 72 hours of transfection (about 24 hours later than after transfection of 293T cells), with a focus formation assay in which the medium from the transfected culture was added to a fresh MDCK cell monolayer, and infectious virus was detected by immunostaining for expressed influenza virus nucleoprotein (NP). After virus amplification in MDCK cells, which generally does not select for HA-adaptive mutations (*16*), we verified HA and NA identity by sequencing HA gene– and NA gene–specific reverse transcription PCR amplicons from the viral cultures and comparing the sequences to those used to program the oligonucleotide synthesis.

Table 1. Error rate in synthesized genes. The improvement in accuracy without error correction from 3% of clones correct when the program started to 25 to 44% of the control clones correct is a result of changes other than enzymatic error correction that also improved accuracy. These other changes include the use of oligonucleotide sets without gaps, the elimination of one PCR, and the elimination of one round of subassembly. The synthesized HA and NA genes are from A/Uruguay/716/2007 (H3N2).

Error correction description	Gene	No. of clones correct	No. of clones analyzed	% Clones correct	No. of bases synthesized	No. of errors	Error rate (1 error per × bp)	Grand total: No. of bases synthesized per method	Grand total: No. of errors	Grand total: Error rate (1 error per × bp)
One round correction	HA	15	16	93.75	28,192	1	28,192	57,532	6	9,589
	NA	16	20	80.00	29,340	5	5,868			
One round control*	HA	4	15	26.67	26,430	22	1,201	55,770	42	1,328
	NA	5	20	25.00	29,340	20	1,467			
Two rounds correction	HA	22	24	91.67	42,288	2	21,144	77,496	3	25,832
	NA	23	24	95.83	35,208	1	35,208			
Two rounds control*	HA	4	9	44.44	15,858	8	1,982	43,731	28	1,562
	NA	8	19	42.11	27,873	20	1,394			

*In the controls for one and two rounds of error correction, the error correction enzymes were omitted from the reactions.

Backbones for synthetic virus rescue

We further increased rescue efficiency by using improved influenza backbones (sets of genome segments encoding influenza virus proteins other than HA and NA) (Fig. 3 and table S1). The initial improvement in the backbone resulted from the use of genes from a PR8 variant (designated PR8x) that had been adapted over five passages to growth in MDCK 33016PF cells. Additional improvements resulted from combining PR8x backbone genome segments with backbone genome segments from biosafety level 2 human influenza isolates that were not highly pathogenic. During pilot manufacturing of influenza vaccines in MDCK 33016PF cells, several human influenza viruses, including strain A/Hessen/105/2007 [an A/New Caledonia/20/1999 (H1N1)–like strain that was isolated in 2007 from a patient without severe disease and then passaged 30 times in MDCK 33016PF cells], were adapted to grow efficiently in MDCK 33016PF cells, although not as efficiently as strain PR8x. Synthesized viruses with HA and NA genes from historical H3N2 strains and all possible backbone combinations of five PR8x genome segments and one A/Hessen/105/2007 genome segment or three PR8x genome segments and three A/Hessen/105/2007 genome segments were screened for virus growth by a focus formation assay and for HA production by an enzyme-linked immunosorbent assay (ELISA). This screen identified a backbone (designated #19), composed of NP, PB1, and PB2 genome segments from strain A/Hessen/105/2007 and M, NS, and PA genome segments from strain PR8x, that often outperformed equivalent viruses with entirely PR8x backbones in reverse genetic rescue efficiency and yield of HA (Table 2, table S1, Fig. 3, and fig. S4, A to D). Similarly, synthesized viruses with HA and NA genes from H1N1 strains and a backbone (designated #21) with the PB1 genome segment of the 2009 H1N1 pandemic strain, A/California/7/2009, and the other genome segments from strain PR8x often had greater rescue efficiencies and HA yields than equivalent viruses with entirely PR8x backbones (Table 2, table S1, Fig. 3, and fig. S4, A to D). This finding is consistent with a report that the A/California PB1 genome segment is preferentially found in the reassortant progeny of co-infections of chicken eggs with A/California/7/2009 and a donor strain that has a PR8 backbone (*17*).

Historically, most influenza type B vaccine seeds have been wild-type viruses, not reassortants, because wild-type influenza B viruses generally provide adequate yields. To use our synthetic procedures for influenza B viruses more readily, we developed two optimized type B backbones that provided consistent rescue of synthetic influenza B viruses (Table 2, table S1, Fig. 3, and fig. S4, E and F). In the first (designated Brisbane), all backbone genome segments originated from B/Brisbane/60/2008 (B/Victoria lineage); in the second (designated B34), the genome segments encoding PA, PB1, PB2, and NP originated from B/Brisbane/60/2008, and those encoding M and NS originated from B/Panama/45/1990 (B/Yamagata lineage).

Overall, the use of optimized backbones for A strains increased rescue efficiencies up to 1000 times (as measured by infectious titers obtained after transfection) (fig. S4, A to D) and increased HA yields in research-scale infections of MDCK 33016PF cells by 0.3 to 9.9 times relative to reference strains, depending on the strain and assay used for HA detection (Table 2). In general, yields of HA from these viruses were also increased relative to those from viruses with PR8 backbones when the viruses were propagated in embryonated chicken eggs (table S2). To make use of such strain-specific differences, an optimal synthetic seed generation strategy would combine the HAs and NAs from circulating strains of interest with a panel of alternative backbones to maximize the chances of isolating a high-yielding vaccine virus.

Synthetic vaccine virus generation in a simulated pandemic response

In a proof-of-concept test of the synthetic system's first iteration, BARDA collaborators not directly involved in the synthesis provided our virus synthesis group with unidentified, partial HA and NA genome segment sequences at 10:09 a.m. EDT on Wednesday, 24 August 2011 (Fig. 4). The sequences included complete coding regions but incomplete

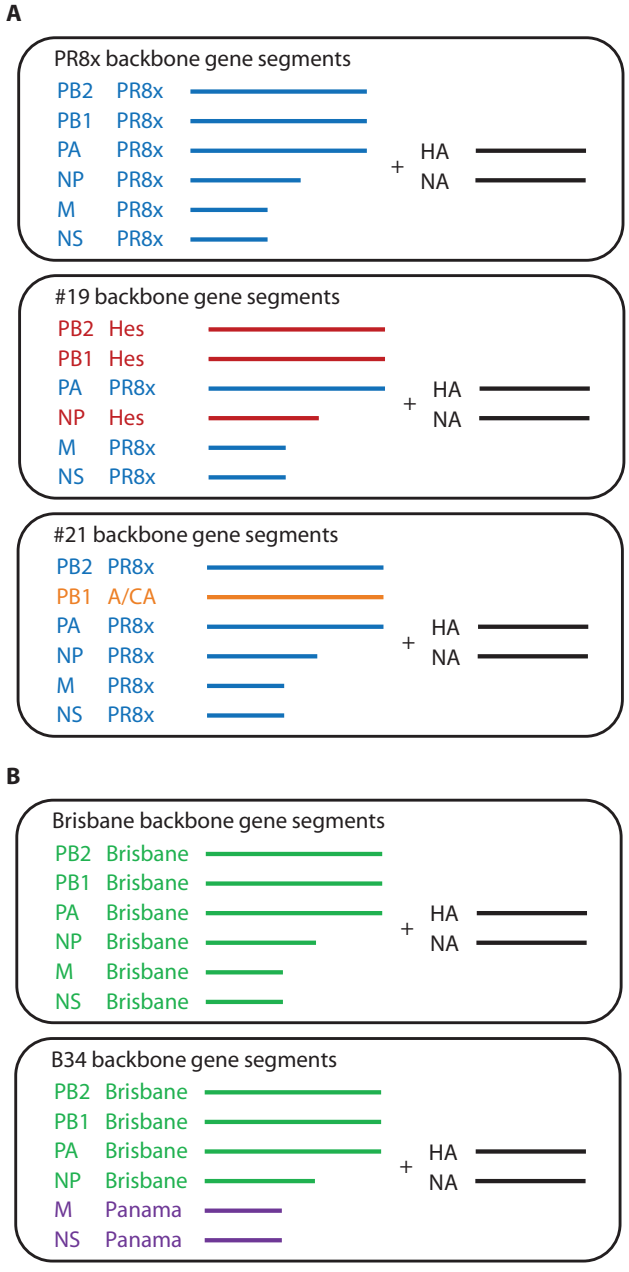

Fig. 3. Panel of backbones used to rescue synthetic influenza viruses. (**A** and **B**) Backbones for (A) type A and (B) type B influenza strains. Synthesized HA and NA genes from circulating strains are matched with backbone genes from plasmids. GenBank accession numbers for backbone gene sequences are listed in table S1. Hes, A/Hessen/105/2007 (H1N1); A/CA, A/California/7/2009 (H1N1); Brisbane, B/Brisbane/60/2008 (Victoria lineage); Panama, B/Panama/45/1990 (Yamagata lineage).

UTRs, mimicking the information likely to be available in the early days of a pandemic. Sequence analysis of the HA genome segment showed that it was very closely related (96% nucleotide sequence identity by Blast to GenBank) to a low-pathogenicity North American avian H7N3 virus (A/Canada goose/BC/3752/2007, GenBank accession code EU500844) and that the NA genome segment was very closely related (96% nucleotide sequence identity by Blast to GenBank) to a low-pathogenicity North American avian H10N9 virus (A/king eider/Alaska/44397-858/2008, GenBank accession code HM060036). Although the HANABOD software generates the sequences of the oligonucleotides for assembly of the synthetic genes, user intervention is needed when there are ambiguities in the available sequence data, such as heterogeneity in the UTRs of fully sequenced genome segments that are similar to a partially sequenced, new HA or NA variant of interest. Heterogeneity in UTRs is found in multiple influenza subtypes. In the test case, the unknown terminal UTR sequences were reconstructed by sequence alignment of the test coding sequences with a limited number of related full-length, high-quality H7 HA genome segment and N9 NA genome segment sequences in GenBank, followed by comparison of the identified UTRs. This analysis revealed heterogeneity in the noncoding regions of NA genes of N9 strains (U/C at 1434 in the positive-sense orientation). So, alternative sets of 5′ NA oligonucleotides were used to construct two variants of the NA cassettes: one containing T at 1434 and one containing C. UTR design was completed at 12.40 p.m. EDT on Wednesday, 24 August 2011 (Fig. 4).

By agreement with BARDA, the timed portion of the test began at a prespecified hour, 8:00 a.m. EDT on Monday, 29 August 2011, when the full-length HA and NA genome segment nucleotide sequences, including reconstructed UTRs, were used as input to a precursor of the HANABOD software program, which generated the oligonucleotide sequences for synthesis (Fig. 4 and tables S4 and S5). By noon on Friday, 4 September, immunostaining of a secondary culture confirmed that the virus had been rescued. The 4 days and 4 hours from start of oligonucleotide design to detection of rescued virus (4 days and 6.5 hours if the time to reconstruct the UTRs is added) included time spent shipping DNA from the oligonucleotide synthesis and gene assembly laboratories in California to the virus rescue laboratory in Massachusetts. If all functions were consolidated in one location, the potential for delays and mishaps from shipping would be reduced.

These original proof-of-concept rescues were conducted with 293T cells; rescue of the strains with MDCK cells, as in an actual pandemic response, slows detection of rescued virus by about 24 hours (fig. S5). The sequences of the HA and NA genome segments of the synthetic H7N9 reassortant viruses from the proof-of-concept exercise were determined after two rounds of virus amplification in MDCK 33016PF cells and were identical to those used to program oligonucleotide synthesis. Two-way hemagglutination inhibition (HI) testing (reciprocal HI assays with antigen from the synthetic and natural strains and ferret sera drawn after synthetic and natural virus infection) (*18*), conducted by the U.S. CDC, demonstrated antigenic identity of the synthetic virus to the source wild-type virus and confirmed that the synthesized virus was immunologically active (Table 3). A/goose/Nebraska/17097-4/2011 (H7N9) (GenBank accession codes JX899805 and JX899806) was subsequently revealed as the source wild-type virus for the sequences that were electronically transmitted to the virus synthesis group.

The A/goose/Nebraska/17097-4/2011 HA and NA genes were rescued with PR8x, #19, and #21 backbones. Virus rescue was more efficient with the #19 and #21 backbones than with the PR8x backbone, based on the titers of viruses harvested 48 and 72 hours after transfection (Fig. 5A). To test growth characteristics, we amplified the synthetic viruses once in MDCK 33016PF monolayers and then used them to infect suspension MDCK 33016PF cultures at a multiplicity of infection of 0.001. Despite differences in the efficiency of virus recovery, viruses exhibited similar growth characteristics, regardless of backbone (Fig. 5B). The H7N9a set of viruses (C1434 positive-sense NA) achieved infectious titers about 10 times higher than their H7N9b counterparts (U1434 positive-sense NA)

Table 2. Virus titers and HA yields from influenza viruses with optimized backbones in MDCK 33016PF cells. Test strain yields are presented as fold improvement over reference strain yields, which are normalized to 1.0. Reference strains were obtained from the U.S. CDC or the UK National Institute for Biological Standards and Control (NIBSC). Reversed-phase high-pressure liquid chromatography (RP-HPLC) or lectin-capture ELISA was used to detect HA from the culture medium of virus-infected cells (multiplicity of infection = 0.001 or 0.0001). n/a, data not available because strain-specific antisera were not available for ELISA; Ref. undetect., data not available because the reference strain had undetectable HA levels by RP-HPLC.

Test strain	Reference strain	HA yield by ELISA		HA yield by RP-HPLC		Best backbones
		Fold increase	*P**	Fold increase	*P**	
H1N1						
A/Christchurch/16/2010	NIB74	4.3	0.0025 (*n* = 8)	2.8	0.0544 (*n* = 5)	#21
A/Brisbane/10/2010	Wild type	6.9	0.0005 (*n* = 13)	4.2	0.1207 (*n* = 5)	#21
A/Brisbane/59/2007	IVR-148	2.9	— (*n* = 1)	1.9	— (*n* = 1)	#21
A/Solomon/3/2006	IVR-145	6.4	— (*n* = 2)	1.8	— (*n* = 1)	#21
H3N2						
A/Victoria/361/2011	IVR-165	1.8	0.1548 (*n* = 4)	1.8	0.0740 (*n* = 4)	PR8x
A/Victoria/210/2009	X187	1.8	0.0299 (*n* = 7)	3.4	0.2741 (*n* = 3)	PR8x
A/Wisconsin/15/2009	X183	9.9	— (*n* = 2)	Ref. undetect.	—	#19
A/Uruguay/716/2007	X175C	1.4	0.0191 (*n* = 7)	1.4	— (*n* = 1)	#19
H5N1						
A/turkey/Turkey/1/2005	NIBRG23	2.1	0.0479 (*n* = 8)	3.8	0.1324 (*n* = 4)	#19, #21†
H3N2v						
A/Indiana/8/2011	X213	n/a	n/a	2.4	0.0005 (*n* = 8)	#21
B Yamagata						
B/Wisconsin/1/2010	Wild type	2.1	0.2502 (*n* = 4)	1.1	0.6266 (*n* = 3)	Brisbane
B/Brisbane/3/2007	Wild type	2.9	— (*n* = 2)	2.0	— (*n* = 2)	#B34
B/Florida/3/2006	Wild type	1.6	0.3892 (*n* = 3)	Not tested	Not tested	#B34
B Victoria						
B/Brisbane/60/2008	Wild type	1.0	0.9555 (*n* = 15)	1.5	0.0088 (*n* = 7)	Brisbane
B/Brisbane/32/2002	Wild type	2.3	0.4060 (*n* = 3)	1.8	0.1813 (*n* = 3)	Brisbane

*Two-tailed *P* values were calculated with a paired *t* test. —, not enough replicates for statistical evaluation; *n*, number of replicates. †For A/turkey/Turkey/1/2005, statistical analyses for HA yields were based on results from viruses with two different backbones and equivalent yields relative to the reference strain.

(fig. S6). The viruses with the highest infectious yields also produced the most HA per volume of infected MDCK suspension culture (Fig. 5, C and D). Thus, the single-nucleotide substitution in the 5′ NA noncoding region of the genomic RNA strongly influenced both infectious titer and HA yield. The H7N9a virus with the #19 backbone produced about 1.5 times more HA than a virus with the same HA and NA in the context of the standard PR8x backbone (Fig. 5, C and D). This result illustrates the importance of rescuing multiple HA or NA variants with multiple backbones to increase the probability of identifying high-yielding vaccine virus strains early in the vaccine seed generation process. Simultaneous rescue of multiple variants is faster and more easily accomplished

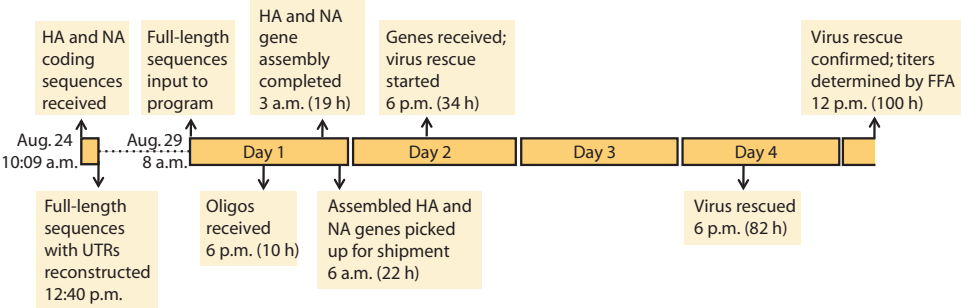

Fig. 4. Timeline of the proof-of-concept synthesis of H7N9 influenza viruses. HA and NA genome segment UTR sequence reconstruction took 2.5 hours and was performed in advance of the timed test. The line from 24 August to 29 August indicates the waiting period from the end of UTR sequence reconstruction to the time set by BARDA for the start of oligonucleotide design and synthesis. The listed times in hours are from the start of processing reconstructed full-length gene segment sequences by a precursor to the HANABOD software program to generate the oligonucleotide sequences for synthesis. FFA, focus formation assay.

Table 3. Confirmation of the antigenic authenticity of synthetic H7N9 viruses by two-way HI testing. HI was performed with turkey red blood cells (RBCs) as described (*18*). Strains with abbreviations listed under both the influenza strains and the antiserum columns were used to inoculate ferrets to generate antisera and as antigen targets for HI, with self-HI reactions in bold. The other strains were used only as antigen targets. Strain origins are synthetic (S) or natural (N). The backbones of the synthetic viruses are listed after their abbreviations and full names. The codes for passage indicate the passage substrate in the first position and the passage number in the second. Passages before arrival at the CDC are left of the backslash; passages at the CDC are on the right. C, MDCK cell–passaged; E, egg-passaged; X, unknown passage number; Norm sheep, normal sheep serum from uninfected, influenza-negative sheep used as a negative control; OK, no RBC agglutination. A PBS control was used to ensure that there was no nonspecific RBC agglutination by the serum.

Influenza strain				Antiserum				
Abbreviations	**Full name**	**Subtype (origin)**	**Passage**	**GS/NE PR8x**	**GS/NE**	**TK/MN**	**TK/VA/4529**	**Norm sheep**
GS/NE PR8x	A/goose/Nebraska/17097-4/2011 PR8x	H7N9 (S)	C2/E1	**320**	640	160	40	<10
GS/NE	A/goose/Nebraska/17097-4/2011	H7N9 (N)	EX/E1	320	**640**	160	40	<10
TK/MN	A/turkey/Minnesota/0141354/2009	H7N9 (N)	EX/E1	80	160	**160**	10	<10
TK/VA/4529	A/turkey/Virginia/4529/2002	H7N2 (N)	E3/E1	160	640	8	**320**	<10
GS/NE #19	A/goose/Nebraska/17097-4/2011 #19	H7N9 (S)	C2/E1	640	1280	640	40	<10
GS/NE #21	A/goose/Nebraska/17097-4/2011 #21	H7N9 (S)	C2/E1	160	640	160	40	<10
H7N9	A/Guinea fowl/Nebraska/17096-1/2011	N7N9 (N)	EX/E1	320	640	640	40	<10
PBS control				OK	OK	OK	OK	OK

with the synthetic approach than standard plasmid mutagenesis approaches. Our results also illustrate the importance, for effective response to pandemics, of including the most complete genome segment sequences possible in genetic databases and of clearly delineating terminal sequences originating from viral genome segments from those originating from sequencing primers.

Robustness of synthetic vaccine virus generation

The synthetic process described here has been used to generate various influenza strains, including H1N1, seasonal H3N2, swine-origin H3N2v, B (Yamagata and Victoria lineages), attenuated H5N1, and H7N9 strains (table S3). To date, we have not encountered any influenza virus strain that cannot be rescued synthetically. The robustness of synthetic influenza virus recovery from MDCK cells is in contrast to the unreliability of conventional vaccine virus isolation using eggs, particularly for recent H3N2 strains (*19*).

DISCUSSION

We have demonstrated that an enzymatic system of gene assembly with error correction lowers error rates sufficiently to allow HA and NA gene cassettes, assembled from chemically synthesized oligonucleotides, to be used to rescue influenza vaccine viruses with prespecified HA and NA sequences and backbones without the need to pause for cloning in *E. coli* and sequencing before transfection (Table 1). The improved fidelity decreased the time from obtaining a sequence to transfecting cells with synthetic HA and NA genes from 4.5 to 5.5 days to less than 1 day (Fig. 2). The reliability of influenza virus rescue in a vaccine manufacturing cell line and yields of HA were increased through the use of improved vaccine backbones (Table 2 and fig. S4). A timed test of vaccine virus synthesis in response to a simulated H7N9 influenza outbreak demonstrated that this process can generate vaccine viruses very rapidly, and the use of this system to rescue diverse synthetic influenza viruses demonstrated the system's robustness. The antigenic equivalence, based on two-way HI testing with ferret infection sera (Table 3), of a synthetic H7N9 vaccine virus and the wild-type H7N9 virus from which the sequence data for synthesis were obtained confirms that the synthetic viral antigens are immunogenic and supports the expectation that vaccines made using synthetic or conventional influenza vaccine viruses will be equivalently protective.

A fast, straightforward, and accurate method of synthesizing higher-yielding influenza vaccine viruses, as described here, could enable more rapid pandemic responses and a more reliable supply of better matched seasonal and pandemic vaccines than available at present. In addition to increasing the speed of gene synthesis and virus rescue, this method also alleviates the need to ship viruses and clinical specimens between laboratories, as well as the requirement for a separate set of viral manipulations, classic reassortment (the "mating" of influenza viruses with stochastic exchange of genome segments during co-infection), to generate high-yielding vaccine strains.

Today, more than 120 National Influenza Centers conduct influenza surveillance and periodically ship clinical specimens to WHO Collaborating Centers, which propagate wild-type viruses in MDCK cells, assess their antigenicity and sequence, reisolate selected viruses in chicken eggs, and reassort them with high-growth backbones. High-growth reassortants recommended by the WHO are then shipped to vaccine manufacturers for further adaptation to make vaccine seed viruses. A system that uses synthetic gene generation could be more efficient. National Influenza Centers could sequence HA and NA genomic RNAs in clinical specimens and post the data on publicly accessible Web sites for immediate download by manufacturers, public health agencies, and researchers worldwide. Continuous comparison of newly posted sequences to databases of sequence and HI data by algorithms now under development could identify the emerging viruses most likely to differ antigenically from current vaccine strains (*20*). Efficient synthetic virus rescue with a panel of high-growth backbones (or alternatively with native backbones, if additional influenza genome segment sequences were provided) could generate simultaneously viruses for antigenic testing and the best vaccine

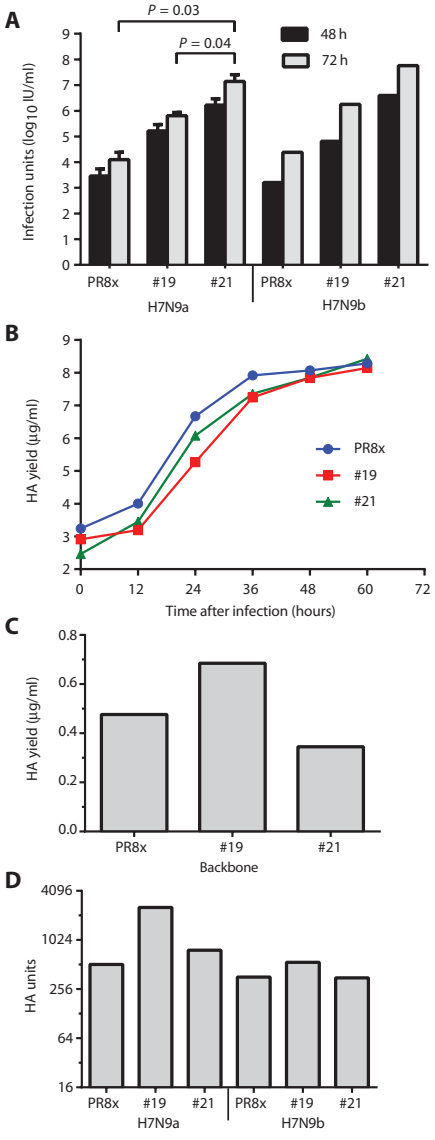

Fig. 5. Performance of synthetic H7N9 reassortant viruses from the proof-of-concept test. (**A**) Titers of influenza viruses synthesized from three alternative backbones and two alternative NA UTRs. The NA UTR in the H7N9a set of viruses has C1434 in the positive sense; the NA UTR in the H7N9b set of viruses has U1434. Culture fluid was harvested from MDCK 33016PF–supplemented 293T cells 48 and 72 hours after cotransfection with the indicated backbone plasmids and synthetic HA and NA gene constructs. Viral titers were determined by a focus formation assay with MDCK cell monolayers. H7N9a data are from three independent experiments; error bars represent the SEM ($n = 3$). One-way analysis of variance (ANOVA), uncorrected Fisher's least significant difference test. H7N9b data are from two independent experiments. (**B**) Replication kinetics of synthetic H7N9a reassortant viruses in MDCK 33016PF suspension cultures. Data are from two independent experiments and are expressed as the mean yield of the two experiments at each time point. (**C**) HA yields from synthetic H7N9 viruses in MDCK suspension cultures, determined by RP-HPLC after purification of viruses on sucrose density gradients. Data are from a single experiment. (**D**) HA yield from synthetic H7N9 viruses in MDCK suspension cultures, as measured by turkey RBC agglutination. Data are from two independent experiments and are expressed as the mean of the values from the two experiments. All measurements in (A) to (D) were made in duplicate.

virus candidates for antigenically distinct strains. The speed and accuracy of gene synthesis by cell-free, enzymatic techniques could also enable more rapid production of the strain-specific genetic constructs used to manufacture recombinant alternatives to conventional influenza vaccines (*21*). Today, vaccine viruses are only shipped to manufacturers after a regimen of testing at WHO-associated laboratories, which often takes longer than actually generating the vaccine strains. Decentralized generation of synthetic viruses could allow manufacturers to undertake scale-up and process development with strains that they generate immediately after the National Influenza Centers post sequences. Carrying out manufacturing activities simultaneously with seed testing could cut additional weeks from pandemic response times. Maintenance of libraries of synthetic influenza genes could further accelerate pandemic responses, if they contain presynthesized genes that match future pandemic strains.

Technical and nontechnical hurdles must be overcome to realize fully the potential benefits of synthetic vaccine viruses for pandemic responses. Research protocols must be translated into performance-tested, at-scale manufacturing processes that have been approved by regulatory authorities. More prompt and open sequence and antigen data sharing is needed, as are biosafety standards for virus synthesis that ensure safety without unduly slowing vaccine production. The efficiency of testing synthetic vaccine viruses must increase. In particular, panels of post-infection ferret sera that react against previous reference viral strains are needed for initial antigenic screening of vaccine viruses, and procedures must be established for decentralized generation of ferret sera against selected synthetic strains for definitive antigenic testing. The current potency assay for vaccine release, which requires a lengthy immunization protocol to generate strain-specific sheep antisera, must be replaced by a more rapid, non–serum-requiring release assay, potentially one based on the physical characteristics of properly folded, immunogenic HA.

Further, the regulatory pathway for strain changes in licensed influenza vaccines must be adapted for synthetic vaccine viruses. Automation could enable access to the technologies needed for a global pandemic response system based on sequencing HA and NA genes in clinical specimens and rapidly synthesizing vaccine viruses.

On 17 April 2009, a new influenza virus strain that had caused outbreaks in Mexico was detected in southern California (*22*, *23*). An initial qualified vaccine virus (X179A) was not received at one of our manufacturing facilities until 29 May, and a vaccine virus (NIBRG-121xp) with ordinary HA yield (10 to 15 mg of HA per 100 eggs) was not received until 21 August, too late to manufacture vaccines for the primary pandemic response (fig. S1) (*2*). If laboratory demonstrations of synthetic vaccine technology such as that reported here prove themselves in manufacturing and field implementation before the next pandemic, a high-yielding vaccine virus could be available to manufacturers for testing, scale-up, and process optimization days, not months, after a new virus is first detected.

MATERIALS AND METHODS

Cells

293T cells were maintained in Dulbecco's modified Eagle's medium (DMEM) (Lonza) containing 10% fetal bovine serum (FBS; Omega Scientific) and penicillin-streptomycin (Lonza) at 37°C with 5% CO_2. Suspension MDCK 33016PF cells were maintained in a shake flask in chemically defined medium (CDM) (Lonza) at 37°C and 5% CO_2 with shaking at 145 rpm. For reverse genetics experiments, six-well plates

were seeded with 293T or MDCK 33016PF cells in DMEM plus 10% FBS and penicillin-streptomycin and were used for transfection when about 70 to 80% confluent.

Design of oligonucleotides

The oligonucleotide sequences used to program chemical synthesis were based on HA and NA gene sequences transmitted via e-mail from BARDA and were designed with a precursor version of the HANABOD software program developed at JCVI (software available in the Supplementary Materials). To design the oligonucleotides, the program initially added set constant regions, "AGTACTGGTCGACCTCCGAAGTTGGGGGGG" and "AATAACCCGGCGGCCCAAAATGCCGACTCG," to the 5′ and 3′ ends, respectively, of a matched pair of HA and NA genes to generate overlaps homologous to the linearized plasmid (pKS10) that provides the genetic control elements to the DNA cassettes used for transfection. The program then divided the HA and NA gene sequences flanking constant regions into oligonucleotide sequences according to a set of rules that minimized the time for chemical synthesis and maximized the reliability of synthesis and subsequent assembly and error correction. These rules were as follows: (i) all bases of both strands are represented, with no unfilled gaps; (ii) the length of the oligonucleotides allows the entire oligonucleotide set for an HA-NA pair to be contained in a single 96-well plate of oligonucleotides; (iii) within an assembly, differences in length between oligonucleotides are limited to 2 bases (for example, 66 to 68 bases) to minimize differences in annealing temperatures; one oligonucleotide of an intermediate length (for example, 67 bases) must bridge the transition between shorter and longer oligonucleotides when the oligonucleotide set is annealed. The length and endpoints of the oligonucleotides are not adjusted on the basis of their nucleotide composition.

Assembly of oligonucleotides into HA and NA gene segments

Overlapping oligonucleotides were pooled for the HA and NA gene segments. For the HA gene segment, 10 μl of each of fifty-two 10 μM oligonucleotides was pooled. For the NA gene segment, 10 μl of each of forty-four 10 μM oligonucleotides was pooled.

The pooled oligonucleotides were assembled with a one-step isothermal assembly protocol. Twenty-microliter reactions were prepared by combining 10 μl of either the pooled HA or NA oligonucleotides with 10 μl of 2× Assembly Mastermix. The 2× Assembly Mastermix was prepared by combining 320 μl of 5× ISO Reaction Buffer [25% polyethylene glycol 8000, 500 mM tris-HCl (pH 8.0), 50 mM $MgCl_2$, 50 mM dithiothreitol (DTT), 1.0 mM each of the four deoxynucleotide triphosphates (dNTPs), 5 mM nicotinamide adenine dinucleotide], 6.4 μl of T5 Exonuclease (1 U/μl) (Epicentre), 20 μl of Phusion polymerase (2 U/μl) [New England Biolabs (NEB)], 80 μl of Taq ligase (40 U/μl) (NEB), and 374 μl of deionized H_2O. The assembly reaction was incubated at 50°C for 30 min. The assembled HA and NA gene segments were amplified with PCR. The PCR mixture contained 5 μl of HA or NA assembly reaction, 71 μl of dH_2O, 20 μl of HF Buffer (NEB), 2 μl of 10 mM dNTPs, 0.5 μl of 100 μM primer BMP_3 (CGAGTCGGCATTTTGGGCCGCCGGGTTATT), 0.5 μl of 100 μM primer BMP_4 (AGTACTGGTCGACCTCCGAAGTTGGGGGGG), and 1 μl of Hot Start Phusion polymerase (NEB). The cycling conditions were 98°C for 60 s; 98°C for 10 s; 60°C for 30 s; 72°C for 1.5 min; go back to step 2 (98°C for 10 s) for 24 additional cycles; then 72°C for 5 min; 98°C for 60 s; 0°C for 5 min; 37°C for 5 min; and 10°C hold.

The HA and NA PCR products were error-corrected with ErrASE (Novici Biotech). Ten microliters of each gene segment was added to each of six wells of an ErrASE kit strip. One strip of six ErrASE wells was required for each gene segment. The error correction reaction was incubated for 60 min at 25°C. To PCR amplify each of the 12 ErrASE wells, we added 2 μl of each ErrASE reaction to 48 μl of PCR Mastermix (36 μl of dH_2O, 10 μl of 5× HF Buffer, 1.0 μl of 10 mM dNTPs, 0.25 μl of 100 μM primer BMP_3, 0.25 μl of 100 μM primer BMP_4, and 0.5 μl of Hot Start Phusion polymerase). The amplification was carried out under the following conditions: 98°C for 60 s; 98°C for 10 s; 60°C for 30 s; 72°C for 1 min and 30 s; go back to step 2 (98°C for 10 s) for 24 additional cycles; then 72°C for 5 min; 10°C hold. The sizes of the gene segments were confirmed on 1.2% E-gels (Invitrogen). DNA bands were visualized and quantitated on an Amersham Typhoon 9410 Fluorescence Imager.

To assemble error-corrected, PCR-amplified HA and NA gene segments into a linear pKS10 plasmid, we added 20 ng of the PCR amplicons to 10 μl of 2× Assembly Mastermix and 0.2 μl of linear pKS10 plasmid (70 ng/μl). Distilled H_2O was added to a total reaction volume of 20 μl. The assembly reaction was incubated at 50°C for 30 min.

Linear HA and NA gene segments were amplified from the circularized plasmids. Thirty replicate PCRs were set up for the HA and the NA gene segments. Each reaction consisted of 5 μl of HA or NA assembled into pKS10 plasmid, 71 μl of dH_2O, 20 μl of 5× HF Buffer, 2.0 μl of 10 mM dNTPs, 0.5 μl of 100 μM primer BMP_13 (CGAAAGGGGGATGTGCTGCAAGGCGA), 0.5 μl of 100 μM primer BMP_14 (CTTCCGGCTCGTATGTTGTGTGGAATTG), and 1 μl of Phusion polymerase. The reactions were amplified under the following conditions: 98°C for 30 s; 98°C for 10 s; 72°C for 2 min and 30 s; go back to step 2 (98°C for 10 s) for 24 additional cycles; then 72°C for 5 min; 10°C hold. The 30 reactions for each of the gene segments were pooled after PCR amplification. The sizes of the gene segments were confirmed on 1.2% E-gels. DNA bands were visualized and quantified on an Amersham Typhoon 9410 Fluorescence Imager.

Final HA and NA amplicons were then phenol-chloroform–extracted and ethanol-precipitated. DNA pellets were dissolved in 50 μl of tris-EDTA buffer (pH 8.0). The final products are uncloned, synthetic linear HA or NA gene segments with regulatory control elements (promoters and terminators).

Reverse genetics

For transfection of 293T cells, 27 μl of FuGENE (Promega) was added to 73 μl of serum-free and antibiotic-free DMEM (Lonza) and incubated at room temperature for 5 min. Plasmid DNA (consisting of 1 μg each of plasmids encoding the six influenza backbone genes PA, PB1, PB2, NP, NS, and M and a helper plasmid encoding the serine protease TMPRSS2) was combined with 1 μg each of synthetic HA and NA linear cDNA before addition of the mixture to the diluted FuGENE. The mixture was then incubated for 20 min at room temperature. Transfection complexes were added directly to a well of a six-well plate containing 1.5×10^6 293T cells in 2 ml of cell-seeding medium (DMEM containing penicillin-streptomycin and 10% FBS) and incubated at 37°C and 5% CO_2. At 18 hours after transfection, the medium was aspirated from each well, and the cells were washed twice with culture medium (serum-free DMEM containing penicillin-streptomycin) and replenished with 2 ml of culture medium containing TrypZean (0.5 μg/ml) (Sigma) and 3×10^5 feeder MDCK 33016PF cells. Cells were incubated for another 2 days before the harvest of transfection supernatants.

To amplify recovered viruses, we initiated a blind passage in which 50 to 500 μl of transfection supernatant was added to a well of a six-well plate containing a confluent monolayer of MDCK 33016PF cells in 2 ml of culture medium containing TrypZean (0.5 μg/ml). For transfection of MDCK 33016PF cells, 1 μg of each DNA was combined as described above followed by the addition of 500 μl of serum- and antibiotic-free DMEM and 10 μl of Plus reagent (Invitrogen) and incubated at room temperature for 5 min. Twenty-five microliters of Lipofectamine LTX (Invitrogen) was then added to the diluted DNA mixture and incubated at room temperature for 30 min. Transfection complexes were directly added to a well of a six-well plate containing 0.6×10^6 MDCK 33016PF cells in 2 ml of cell-seeding medium. The rest of the protocol is identical to that described above.

Propagation of virus in MDCK cells

Ten milliliters of suspension MDCK 33016PF cultures (1×10^6 cells/ml) in propagation medium [70% protein-free medium (Invitrogen), 30% spent CDM (Lonza), TrypZean (0.5 μg/ml) (Sigma)] was inoculated with virus at a multiplicity of infection of 0.001 and incubated in a flask at 34°C and 5% CO_2 with shaking at 145 rpm. Samples were taken at 0, 12, 24, 36, 48, and 60 hours after infection and frozen at −80°C until used to titer viruses and to test for RBC agglutination activity.

Propagation of virus in embryonated chicken eggs

Nine-day-old, specific pathogen–free, embryonated chicken eggs (Charles River) were incubated at 35°C in 70% humidity for 2 days. Eleven-day-old eggs were inoculated with 200 μl of virus diluted in Dulbecco's phosphate-buffered saline (PBS, Invitrogen), typically at a virus dose ranging from 28 to 2800 infectious units per egg. Inoculated eggs were incubated at 35°C, 70% humidity for 72 hours. Eggs were placed at 4°C for 14 to 24 hours before the allantoic fluid was harvested. Allantoic fluid was clarified by centrifugation at 3000 rpm for 5 min, and samples were assayed for viral infectious titer and hemagglutination activity.

Focus formation assay

In a slight modification of a previously described focus formation assay (*24*), samples of culture medium were cleared at 10,000 rpm for 1.5 min in a microcentrifuge. A 10-fold serial dilution was performed on cleared samples with DMEM containing 1% FBS and 1× penicillin-streptomycin as diluent. Diluted samples were added to confluent MDCK monolayers in a 96-well plate and incubated at 37°C and 5% CO_2. After 16 to 18 hours, the supernatant was aspirated, and the cells were washed once with PBS and fixed with a 1:1 mixture of acetone-methanol for 30 min at −20°C. After fixation, the supernatant was aspirated and the cells were washed once with PBST (PBS plus 0.1% Tween 20) and blocked with PBS plus 2% bovine serum albumin (BSA) for 30 min at room temperature. After removal of the blocking buffer, 50 μl of a mixture of mouse monoclonal antibodies recognizing influenza NP (Millipore) diluted 1:6000 in blocking buffer was added to each well and incubated for 1 hour at room temperature. Wells were washed three times with PBST, and 50 μl of goat anti-mouse immunoglobulin G (IgG) (Jackson ImmunoResearch) diluted 1:2000 in blocking buffer was added to each well and incubated for 1 hour at room temperature. Cells were washed three times with PBST, and 50 μl of TrueBlue peroxidase substrate [Kirkegaard and Perry Laboratories Inc. (KPL)] was added to each well and incubated for 5 min at room temperature. Wells were washed one time with distilled water and dried, and the number of blue cells was counted under a microscope.

Sucrose density gradient separation

Sixty milliliters of suspension MDCK 33016PF cultures (1×10^6 cells/ml) in propagation medium was inoculated with virus at a multiplicity of infection of 0.001 and incubated in a flask at 34°C and 5% CO_2 with shaking at 145 rpm. Medium samples were harvested at 60 hours after infection by centrifugation at 1000*g* for 5 min. Forty milliliters of the harvested media was concentrated 20-fold by ultrafiltration (Vivaspin 20 with 300-kD molecular weight cutoff, Sartorius-Stedim Biotech). A continuous sucrose density gradient, consisting of 20 to 60% sucrose in PBS (pH 7.5), was prepared in an open-top polyclear centrifuge tube (Seton Scientific) with a gradient maker (BiºComp). A 1.8-ml sample of the concentrated virus was overlaid on top of the sucrose gradient and centrifuged in the Beckman Coulter Optima L-100 XP Ultra at 100,000*g* for 4 hours. After centrifugation, sucrose gradients were fractionated (about 1 ml per fraction) into 96-well deep well plates. A hemagglutination assay with 0.5% guinea pig RBCs (Cleveland Scientific) was performed on all fractions to determine fractions with the most concentrated virus. Virus-containing fractions were verified by SDS–polyacrylamide gel electrophoresis and pooled.

HA ELISA

Ninety-six–well plates were coated overnight with *Galanthus nivalis* lectin (Sigma). Plates were washed four times with wash buffer (PBS + 0.05% Tween 20) and blocked with blocking buffer [10 mM tris-HCl, 150 mM NaCl, 3% sucrose, 1% BSA (pH 7.68)] for 1 hour at room temperature. Threefold serial dilutions of the samples containing a final concentration of 1% Zwittergent 3-14 (Sigma) were prepared, added in duplicate to the plates, and incubated at 37°C for 30 min in a shaker. After incubation, biotinylated IgG purified from pooled sheep antisera (NIBSC) raised against specific virus strains was added and further incubated at 37°C for 30 min in a shaker. Plates were then washed four times with wash buffer and incubated with streptavidin-alkaline phosphatase (KPL) in wash buffer at 37°C for 30 min in a shaker. Plates were washed four times with wash buffer and developed using *p*-nitrophenyl phosphate (1 mg/ml) (Sigma) in DEA buffer phosphatase substrate (KPL). Plates were read after 40 to 50 min of incubation in the dark at 405 nm with an Infinite 200 PRO plate reader (Tecan).

Reversed-phase high-pressure liquid chromatography

Each 225-μl virus sample was mixed with 25 μl of 10% Zwittergent 3-14 (Sigma) for a final detergent concentration of 1% by gently pipetting, followed by incubation at room temperature for 30 min. Next, 7.5 μl of 1 M DTT was added (for a final concentration of 25 μM) and mixed by gentle pipetting. Samples were heated at 90°C for 10 min, cooled at room temperature for 5 min, and then spun down briefly to remove condensation. For each run, a 100-μl sample was injected onto a POROS R1/10 column (2.1 mm × 100 mm, Applied Biosystems), and HA1 was eluted with a 30 to 35% acetonitrile gradient containing 0.1% trifluoroacetic acid. The HA1 concentration was quantified with purified HA as reference.

Statistics

All statistical evaluations were performed with GraphPad Prism version 5.00 for Windows (GraphPad Software). One-way ANOVA followed by uncorrected Fisher's least significant difference test was used to analyze data sets with three or more groups. A paired *t* test was used to analyze data sets with two groups.

SUPPLEMENTARY MATERIALS

www.sciencetranslationalmedicine.org/cgi/content/full/5/185/185ra68/DC1
Fig. S1. Timelines to the availability of influenza vaccine viruses at manufacturing sites.
Fig. S2. Timelines for synthetic and conventional reverse genetic influenza virus rescue.
Fig. S3. Effect of MDCK feeder cell addition on titers of viruses recovered from DNA-transfected cells.
Fig. S4. Effect of optimized backbones on synthetic influenza virus rescue efficiencies.
Fig. S5. Synthetic H7N9a virus rescue efficiency from MDCK-supplemented 293T cells or from MDCK cells only.
Fig. S6. Replication kinetics of synthetic H7N9 viruses with alternative NA UTRs and different backbones.
Table S1. GenBank accession codes of backbone gene sequences.
Table S2. Virus titers and HA yields from influenza viruses with optimized backbones relative to conventional vaccine viruses when propagated in embryonated chicken eggs.
Table S3. Diversity of synthetic influenza virus strains rescued.
Table S4. Oligonucleotide sequences for HA gene assembly in the proof-of-concept test.
Table S5. Oligonucleotide sequences for NA gene assembly in the proof-of-concept test.
HANABOD (HA and NA BARDA Oligo Designer) software, version 5.2, and documentation.

REFERENCES AND NOTES

1. M. Tizzoni, P. Bajardi, C. Poletto, J. J. Ramasco, D. Balcan, B. Gonçalves, N. Perra, V. Colizza, A. Vespignani, Real-time numerical forecast of global epidemic spreading: Case study of 2009 A/H1N1pdm. *BMC Med.* **10**, 165 (2012).
2. J. S. Robertson, C. Nicolson, R. Harvey, R. Johnson, D. Major, K. Guilfoyle, S. Roseby, R. Newman, R. Collin, C. Wallis, O. G. Engelhardt, J. M. Wood, J. Le, R. Manojkumar, B. A. Pokorny, J. Silverman, R. Devis, D. Bucher, E. Verity, C. Agius, S. Camuglia, C. Ong, S. Rockman, A. Curtis, P. Schoofs, O. Zoueva, H. Xie, X. Li, Z. Lin, Z. Ye, L. M. Chen, E. O'Neill, A. Balish, A. S. Lipatov, Z. Guo, I. Isakova, C. T. Davis, P. Rivailler, K. M. Gustin, J. A. Belser, T. R. Maines, T. M. Tumpey, X. Xu, J. M. Katz, A. Klimov, N. J. Cox, R. O. Donis, The development of vaccine viruses against pandemic A(H1N1) influenza. *Vaccine* **29**, 1836–1843 (2011).
3. E. E. Verity, S. Camuglia, C. T. Agius, C. Ong, R. Shaw, I. Barr, D. Middleton, S. Rockman, Rapid generation of pandemic influenza virus vaccine candidate strains using synthetic DNA. *Influenza Other Respi. Viruses* **6**, 101–109 (2012).
4. T. Strecker, J. Uhlendorff, S. Diederich, C. Lenz-Bauer, H. Trusheim, B. Roth, L. Kolesnikova, C. Aepinus, R. Dornow, J. Gerlach, M. Matrosovich, U. Valley, M. Eickmann, S. Becker, Exploring synergies between academia and vaccine manufacturers: A pilot study on how to rapidly produce vaccines to combat emerging pathogens. *Clin. Chem. Lab. Med.* **50**, 1275–1279 (2012).
5. A. Doroshenko, S. A. Halperin, Trivalent MDCK cell culture-derived influenza vaccine Optaflu (Novartis Vaccines). *Expert Rev. Vaccines* **8**, 679–688 (2009).
6. D. G. Gibson, H. O. Smith, C. A. Hutchison III, J. C. Venter, C. Merryman, Chemical synthesis of the mouse mitochondrial genome. *Nat. Methods* **7**, 901–903 (2010).
7. D. G. Gibson, L. Young, R. Y. Chuang, J. C. Venter, C. A. Hutchison III, H. O. Smith, Enzymatic assembly of DNA molecules up to several hundred kilobases. *Nat. Methods* **6**, 343–345 (2009).
8. P. Suphaphiphat, M. Franti, A. Hekele, A. Lilja, T. Spencer, E. Settembre, G. Palmer, S. Crotta, A. B. Tuccino, B. Keiner, H. Trusheim, K. Balabanis, M. Sackal, M. Rothfeder, C. W. Mandl, P. R. Dormitzer, P. W. Mason, Mutations at positions 186 and 194 in the HA gene of the 2009 H1N1 pandemic influenza virus improve replication in cell culture and eggs. *Virol. J.* **7**, 157 (2010).
9. E. Hoffmann, G. Neumann, Y. Kawaoka, G. Hobom, R. G. Webster, A DNA transfection system for generation of influenza A virus from eight plasmids. *Proc. Natl. Acad. Sci. U.S.A.* **97**, 6108–6113 (2000).
10. C. Nicolson, D. Major, J. M. Wood, J. S. Robertson, Generation of influenza vaccine viruses on Vero cells by reverse genetics: An H5N1 candidate vaccine strain produced under a quality system. *Vaccine* **23**, 2943–2952 (2005).
11. H. Ozaki, E. A. Govorkova, C. Li, X. Xiong, R. G. Webster, R. J. Webby, Generation of high-yielding influenza A viruses in African green monkey kidney (Vero) cells by reverse genetics. *J. Virol.* **78**, 1851–1857 (2004).
12. J. Heix, I. Grummt, Species specificity of transcription by RNA polymerase I. *Curr. Opin. Genet. Dev.* **5**, 652–656 (1995).
13. Z. Wang, G. M. Duke, Cloning of the canine RNA polymerase I promoter and establishment of reverse genetics for influenza A and B in MDCK cells. *Virol. J.* **4**, 102 (2007).
14. P. Suphaphiphat, B. Keiner, H. Trusheim, S. Crotta, A. B. Tuccino, P. Zhang, P. R. Dormitzer, P. W. Mason, M. Franti, Human RNA polymerase I-driven reverse genetics for influenza A virus in canine cells. *J. Virol.* **84**, 3721–3725 (2010).
15. E. Böttcher, T. Matrosovich, M. Beyerle, H. D. Klenk, W. Garten, M. Matrosovich, Proteolytic activation of influenza viruses by serine proteases TMPRSS2 and HAT from human airway epithelium. *J. Virol.* **80**, 9896–9898 (2006).
16. J. M. Katz, M. Wang, R. G. Webster, Direct sequencing of the HA gene of influenza (H3N2) virus in original clinical samples reveals sequence identity with mammalian cell-grown virus. *J. Virol.* **64**, 1808–1811 (1990).
17. A. A. Fulvini, M. Ramanunninair, J. Le, B. A. Pokorny, J. M. Arroyo, J. Silverman, R. Devis, D. Bucher, Gene constellation of influenza A virus reassortants with high growth phenotype prepared as seed candidates for vaccine production. *PLoS One* **6**, e20823 (2011).
18. A. Klimov, A. Balish, V. Veguilla, H. Sun, J. Schiffer, X. Lu, J. M. Katz, K. Hancock, Influenza virus titration, antigenic characterization, and serological methods for antibody detection. *Methods Mol. Biol.* **865**, 25–51 (2012).
19. X. Xu and R. Donis, personal communication.
20. T. B. Stockwell, personal communication.
21. P. R. Dormitzer, T. F. Tsai, G. Del Giudice, New technologies for influenza vaccines. *Hum. Vaccin. Immunother.* **8**, 45–58 (2012).
22. C. Fraser, C. A. Donnelly, S. Cauchemez, W. P. Hanage, M. D. Van Kerkhove, T. D. Hollingsworth, J. Griffin, R. F. Baggaley, H. E. Jenkins, E. J. Lyons, T. Jombart, W. R. Hinsley, N. C. Grassly, F. Balloux, A. C. Ghani, N. M. Ferguson, A. Rambaut, O. G. Pybus, H. Lopez-Gatell, C. M. Alpuche-Aranda, I. B. Chapela, E. P. Zavala, D. M. Guevara, F. Checchi, E. Garcia, S. Hugonnet, C. Roth; WHO Rapid Pandemic Assessment Collaboration, Pandemic potential of a strain of influenza A (H1N1): Early findings. *Science* **324**, 1557–1561 (2009).
23. Centers for Disease Control and Prevention (CDC), Swine influenza A (H1N1) infection in two children—Southern California, March–April 2009. *MMWR Morb. Mortal. Wkly. Rep.* **58**, 400–402 (2009).
24. Y. Okuno, K. Tanaka, K. Baba, A. Maeda, N. Kunita, S. Ueda, Rapid focus reduction neutralization test of influenza A and B viruses in microtiter system. *J. Clin. Microbiol.* **28**, 1308–1313 (1990).
25. http://platform.gisaid.org
26. B. Zhou, M. E. Donnelly, D. T. Scholes, K. St George, M. Hatta, Y. Kawaoka, D. E. Wentworth, Single-reaction genomic amplification accelerates sequencing and vaccine production for classical and swine origin human influenza A viruses. *J. Virol.* **83**, 10309–10313 (2009).

Acknowledgments: We thank N. Cox, R. Donis, X. Xu, and their colleagues at the Influenza Division of the U.S. CDC for providing influenza RNA for the 2009 synthesis of the recombinant vaccine seed, for providing the unknown influenza gene sequences for the simulated pandemic response, for conducting two-way HI testing of the synthetic H7N9 virus, and for providing advice and helpful discussions. We thank J. McCauley and his colleagues at the WHO Influenza Centre at the Medical Research Council National Institute for Medical Research in London, I. Barr and his colleagues at the WHO Collaborating Centre for Reference and Research on Influenza at the Victorian Infectious Diseases Reference Laboratory in Melbourne, and D. Bucher and her colleagues at the Department of Microbiology and Immunology at the New York Medical College in Valhalla for advice and helpful discussions. We thank W. Wang and A. Subba for their expert technical assistance in virus titration, sequencing, and antigenic analysis at JCVI. JCVI has partnered with the U.S. NIH Genome Sequencing Centers to sequence the diversity of influenza genomes circulating in humans and animals and to synthesize a library of influenza glycoprotein genes representing antigenic variants from multiple subtypes. **Funding:** Supported in part by BARDA contract HHSO100201000061C and by funds from the Novartis Foundation. The influenza virus sequence database used for UTR construction and the generation of a library of synthetic gene segments was funded in part by the National Institute of Allergy and Infectious Diseases, NIH, Department of Health and Human Services under contract number HHSN272200900007C. **Author contributions:** P.R.D. conceived and directed the project, managed and designed the experiments, interpreted the data, and contributed to the manuscript; P.S. designed and carried out the experiments, interpreted the data, and contributed to the manuscript; D.E.W. led viral studies, managed and designed the experiments, and contributed to the manuscript; E.A.D., D.G.G., M.A.A., N.A., J.Z., and D.M.B. developed DNA synthesis methods and performed DNA synthesis; M.B., A.D., and B.M.D. provided scientific advice and guidance on integration with the flu surveillance and strain change network; S.C. carried out virus rescue and backbone development experiments; I.D.S. did experiments to optimize virus rescue on MDCK cells; V.G.D. aided in synthetic experimental design and gene construction; S.B., M.E., M.M., and T. Strecker oversaw virus rescue optimization experiments during the 2009 pandemic; R.C.G. carried out backbone development experiments; C.M. and T.B.S. developed informatics used for synthetic DNA construct design; G.P. designed and oversaw assay experiments and interpreted the data; G.A.P. managed the project; A.F., C.J., L.H., S.M., T. Spencer, and Y.W. designed and carried out virus and HA assay experiments; H.T. and J.U. carried out virus rescue optimization during the 2009 pandemic and provided scientific advice; A.C.Y. aided DNA synthesis; B.Z. performed virologic experiments; P.W.M. led and designed rescue, backbone, and assay experiments, interpreted the data, and contributed to the manuscript; J.I.G. led the synthetic component of the project, managed and designed the experiments, and contributed to the manuscript; and R.R. and J.C.V. conceived and oversaw the synthetic vaccinology collaboration. **Competing interests:** P.R.D., P.S., S.C., I.D.S., A.F., R.C.G., L.H.,

C.J., S.M., G.P., G.A.P., T. Spencer, H.T., Y.W., P.W.M., and R.R. are employees of or contractors for NV&D, which manufactures and sells influenza vaccines; P.R.D., P.S., G.P., G.A.P., H.T., Y.W., P.W.M., and R.R. are Novartis shareholders. The findings and conclusions in this report are those of the authors and do not necessarily represent the views of the Department of Health and Human Services or its components. **Data and materials availability:** GenBank accession codes are provided in table S1 or as listed in the text. Requests for materials will be accommodated with material transfer agreements. The technology and the material discussed in this paper are protected by various patents owned or controlled by Novartis AG, Synthetic Genomics Inc., or MedImmune Inc., including patents on reverse genetics methods for virus rescue and on optimized influenza backbones. The U.S. government has certain rights under these patents. Commercial use of the technology or the material requires a license from the patent holders. The HANABOD software program is available in the Supplementary Materials.

Submitted 16 April 2013
Accepted 2 May 2013
Published 15 May 2013
10.1126/scitranslmed.3006368

Citation: P. R. Dormitzer, P. Suphaphiphat, D. G. Gibson, D. E. Wentworth, T. B. Stockwell, M. A. Algire, N. Alperovich, M. Barro, D. M. Brown, S. Craig, B. M. Dattilo, E. A. Denisova, I. De Souza, M. Eickmann, V. G. Dugan, A. Ferrari, R. C. Gomila, L. Han, C. Judge, S. Mane, M. Matrosovich, C. Merryman, G. Palladino, G. A. Palmer, T. Spencer, T. Strecker, H. Trusheim, J. Uhlendorff, Y. Wen, A. C. Yee, J. Zaveri, B. Zhou, S. Becker, A. Donabedian, P. W. Mason, J. I. Glass, R. Rappuoli, J. C. Venter, Synthetic generation of influenza vaccine viruses for rapid response to pandemics. *Sci. Transl. Med.* **5**, 185ra68 (2013).

Science Translational Medicine
AAAS

Synthetic Generation of Influenza Vaccine Viruses for Rapid Response to Pandemics

Philip R. Dormitzer, Pirada Suphaphiphat, Daniel G. Gibson, David E. Wentworth, Timothy B. Stockwell, Mikkel A. Algire, Nina Alperovich, Mario Barro, David M. Brown, Stewart Craig, Brian M. Dattilo, Evgeniya A. Denisova, Ivna De Souza, Markus Eickmann, Vivien G. Dugan, Annette Ferrari, Raul C. Gomila, Liqun Han, Casey Judge, Sarthak Mane, Mikhail Matrosovich, Chuck Merryman, Giuseppe Palladino, Gene A. Palmer, Terika Spencer, Thomas Strecker, Heidi Trusheim, Jennifer Uhlendorff, Yingxia Wen, Anthony C. Yee, Jayshree Zaveri, Bin Zhou, Stephan Becker, Armen Donabedian, Peter W. Mason, John I. Glass, Rino Rappuoli and J. Craig Venter (May 15, 2013)
Science Translational Medicine **5** (185), 185ra68. [doi: 10.1126/scitranslmed.3006368]

Editor's Summary

Fast, Faster, Fastest

Unlike the public health successes of polio and smallpox vaccines, the flu vaccine has not been so effective. Part of the reason is that there are thousands of influenza virus strains and they evolve rapidly, even to the point of switching hosts, most alarmingly from animals to humans. To keep up with this ever-evolving target, a new flu vaccine is manufactured every year. However, the conventional process is slow, requiring isolation of the flu virus, cloning or reassortment steps and bulk growth in eggs, so that by the time the vaccine is available for use, the circulating flu virus is different or, worse, in the case of a pandemic, the peak of disease incidence is past. Now, Dormitzer *et al.* have streamlined the process considerably by synthesizing the genes needed for the vaccine directly from the sequence and designing more productive vaccine viruses. In a simulated response to a pandemic with a H7N9 bird flu —similar to the one that has recently killed numerous people in China—they show that their new procedure could shave weeks off the time needed for vaccine manufacture and put us in a much better position to respond quickly to a sudden pandemic.

The authors started with the gene sequences for the two flu proteins needed for the vaccine: hemagglutinin and neuraminidase. A custom software program calculated the sequences of needed oligonucleotides; these were generated and then the genes were built enzymatically in cell-free reactions that also included a critical error correction step. Transfection of these synthetic genes into Madin-Darby canine kidney cells, along with an assortment of improved flu backbones that coded for the other necessary viral genes, allowed the authors to select the combination that yielded the most vaccine antigen. Inoculation of ferrets with the synthetic vaccine virus produced the same immune reaction as did the natural virus.

Although the process will still need to be optimized further—it must perform in a large-scale manufacturing setting—the greatest remaining bottleneck is to convince the regulatory agencies that the method is safe and effective.

Science Translational Medicine (print ISSN 1946-6234; online ISSN 1946-6242) is published weekly, except the last week in December, by the American Association for the Advancement of Science, 1200 New York Avenue, NW, Washington, DC 20005.

Science Translational Medicine (print ISSN 1946-6234; online ISSN 1946-6242) is published weekly, except the last week in December, by the American Association for the Advancement of Science, 1200 New York Avenue, NW, Washington, DC 20005.